



Research paper

Evolution of the Northern Nicaragua Rise during the Oligocene–Miocene: Drowning by environmental factors

Maria Mutti^{a,*}, André W. Droxler^b, Andrew D. Cunningham^c

^a*Institut für Geowissenschaften, Universität Potsdam, Postfach 60 15 53, Potsdam D-14415, Germany*

^b*Rice University, Department of Earth Science, P.O. Box 1892, Houston, TX 77251-1892, USA*

^c*BP Amoco, 501 Westlake Park Boulevard, Houston, TX 77253-3092, USA*

Received 16 June 2004; received in revised form 14 December 2004; accepted 20 December 2004

Abstract

Possible causes to explain platform drowning have been hotly debated by carbonate sedimentologists for more than a decade now. In this paper, we present multiple evidence to explain the drowning of a carbonate megabank that covered most of the modern Northern Nicaragua Rise (NNR) during an interval spanning from late Oligocene to early Miocene by the interaction of several environmental factors. The recovery during ODP Leg 165 of late Oligocene to middle Miocene sedimentary sequences in the sub-seafloor of the modern channels and basin, Pedro Channel and Walton Basin, respectively, that dissect the NNR (Site 1000) and south of the rise in the Colombian Basin (Site 999), combined with information from dredged rock samples, allows us to explore in more detail the timing and possible mechanisms responsible for the drowning of the megabank and its relationship to Miocene climate change. The modern system of isolated banks and shelves dissected by a series of intervening seaways and basins on the NNR has evolved from a continuous, shallow-water carbonate “megabank” that extended from the Honduras/Nicaraguan mainland to the modern island of Jamaica. Available information suggests that this megabank broke apart and partially drowned in the late part of the late Oligocene at around 27 Ma and finally foundered during the late early Miocene around 20 Ma, resulting in limited neritic coral growth in the areas where the modern isolated carbonate banks and shelves are occurring today. Available information also suggests that the southern and central parts of Pedro Channel were already a deep-water area before the major episode of platform drowning, and its formation predates the initiation of the Caribbean Current. However, after the partial drowning of the megabank, the channel has become a major pathway for the Caribbean Current. Stratigraphic units identified in deep-water carbonates sampled at ODP Sites 999 and 1000 help to constrain the environmental setting leading to the drowning of the banks. Changes in lithology and mass accumulation rates of both the carbonate and non-carbonate fraction parallel stable isotope shifts and likely indicate regional changes in climate and circulation during the late Oligocene–middle Miocene interval. Carbonate mass accumulation rates (MARs) at Site 999 suggest increased regional productivity during the early Miocene. Terrigenous MARs at both Sites 999 and 1000 show a general increase from the Burdigalian through the Serravallian. The temporal association among episodes of neritic platform deposition, followed by increased productivity as identified by higher

* Corresponding author.

E-mail addresses: mmutti@geo.uni-potsdam.de (M. Mutti), andre@rice.edu (A.W. Droxler).

carbonate MARs and positive excursion in carbon isotopes, suggests that oceanographic changes such as local upwelling and nitrification have led to the partial drowning of the NNR “megabank”.

© 2005 Elsevier B.V. All rights reserved.

Keywords: Northern Nicaragua Rise; Oligocene–Miocene; Drowning

1. Introduction

The stratigraphic record comprises many cases of drowned platforms (Schlager, 1981; Hallock and Schlager, 1986). This occurrence constitutes a scientific paradox, as the growth potential of platforms exceeds the rates of sea-level rise available for drowning. Since the identification of the drowning paradox (Schlager, 1981), carbonate sedimentologists have hotly debated what processes can cause platform drowning. Recently, Schlager (1999) has demonstrated that the growth potential of carbonate platforms follows a scaling trend. The long-term (million-year) drowning of carbonate platforms requires that the reduction of growth during long time scales is largely caused by environmental factors. It has been demonstrated in Jurassic settings that platform drowning is associated with abrupt shallow facies changes (Bloemer and Reijmer, 1999) and, based on fluid inclusion paleobarometry, that water depth has increased at slower rates than normal platform growth (Mallarino et al., 2002). These findings require environmental changes for platform drowning. However, no known cases so far have directly demonstrated changes in the ocean environment concomitant to drowning episodes. In this paper, we present multiple lines of evidence for the gradual and partial drowning of a large carbonate platform (megabank) that covered the modern Northern Nicaraguan Rise (NNR) on its entire length from the late Oligocene until the late early Miocene by the interaction of several environmental factors.

The carbonate platforms of the NNR (see Fig. 1) provide a modern example of a carbonate system where oceanography plays an important role on biotic assemblages and stratal architecture. The NNR platforms, banks, and shelves, despite being located in tropical waters remote from terrigenous influx, are relatively deep and support almost no coral-reef development (Hallock and Elrod, 1988;

Hallock et al., 1988; Hine et al., 1988). Hallock et al. (1988) suggested that intermediate trophic resources, resulting from topographic-induced upwelling, sustain algal–sponge dominated benthic communities with *Halimeda* bioherms (Hine et al., 1988) rather than coral–algal dominated reef systems as found in the Bahamas (e.g., Illing, 1954). In addition, sediment accumulation on the bank and shelf tops has been strongly influenced by some strong ocean surface currents (Caribbean Current) whereas the easterly winds play a secondary role in winnowing the fine sediments produced on the bank and shelf tops and preferentially dumping those on a down current instead of down wind directions, leaving a thin cover of coarse sediments on the bank and shelf tops (Hine et al., 1988; Glaser and Droxler, 1993).

Based on the interpretation of a high-resolution seismic grid and analyses of dredged shallow-water limestones cropping out on the sea-floor, Droxler et al. (1992) showed that the modern system of banks, seaways, and basins on top of the NNR have evolved from a continuous, shallow-water carbonate megabank that extended from the Caribbean shelf of Honduras and Nicaragua and the western and central part of the Jamaica mainland, and suggested that this megabank broke apart and partially foundered in the middle Miocene (Figs. 2 and 3). It is postulated that the partial foundering of the megabank led to the opening of this major intra-Caribbean gateway and to the initiation and evolution of the Caribbean Current and thus contributed at that time to the intensification of the Gulf Stream (Droxler et al., 1998). It has been suggested that the foundering of the NNR megabank was possibly related to a reorganization of the spreading within the Cayman Trough as a result of extensional forces created by changing tectonic activity in the boundary zone between the North American and Caribbean plates (Droxler et al., 1992, 1998; Duncan et al., 1999).

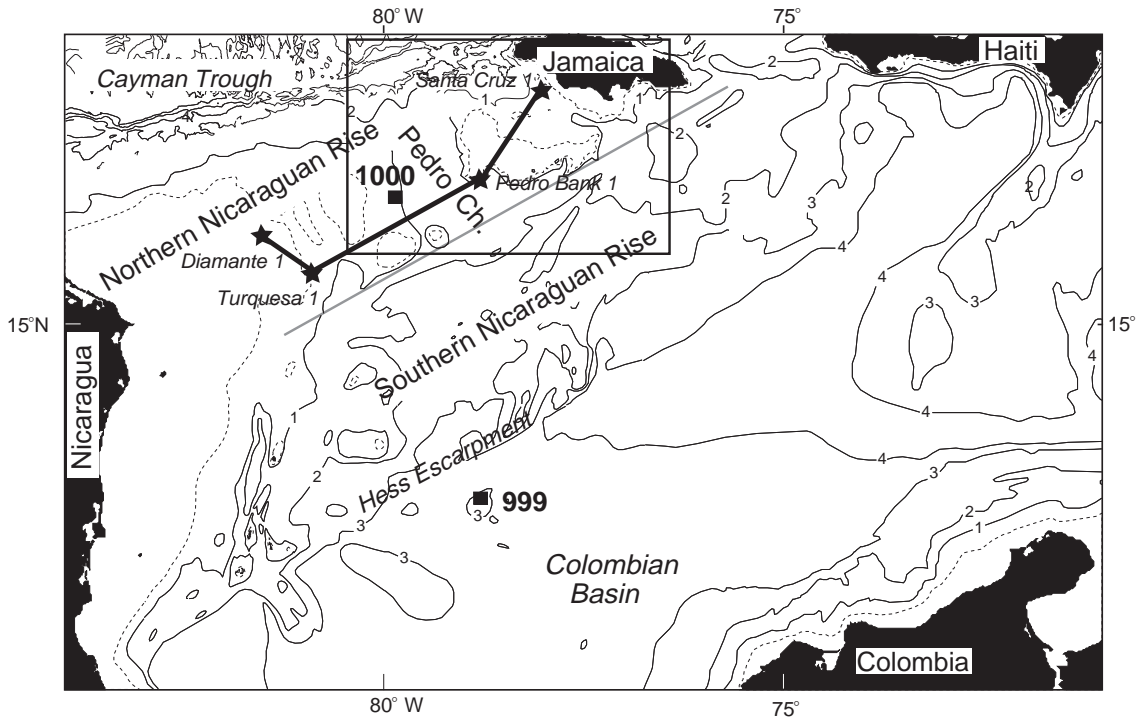


Fig. 1. Bathymetric map showing the location of Northern and Southern Nicaraguan Rise, separated by the Pedro Fault Zone (marked by the gray line), Pedro Channel, and ODP Sites 999 and 1000 in the Caribbean. The solid isobath lines indicate 1 km depth increments; the hatched line marks the 500-m depth. The small stars indicate the location (and, in italics, the name) of the industrial wells illustrated in Fig. 2, connected by the thicker black line. The rectangle indicates the area illustrated in Fig. 3.

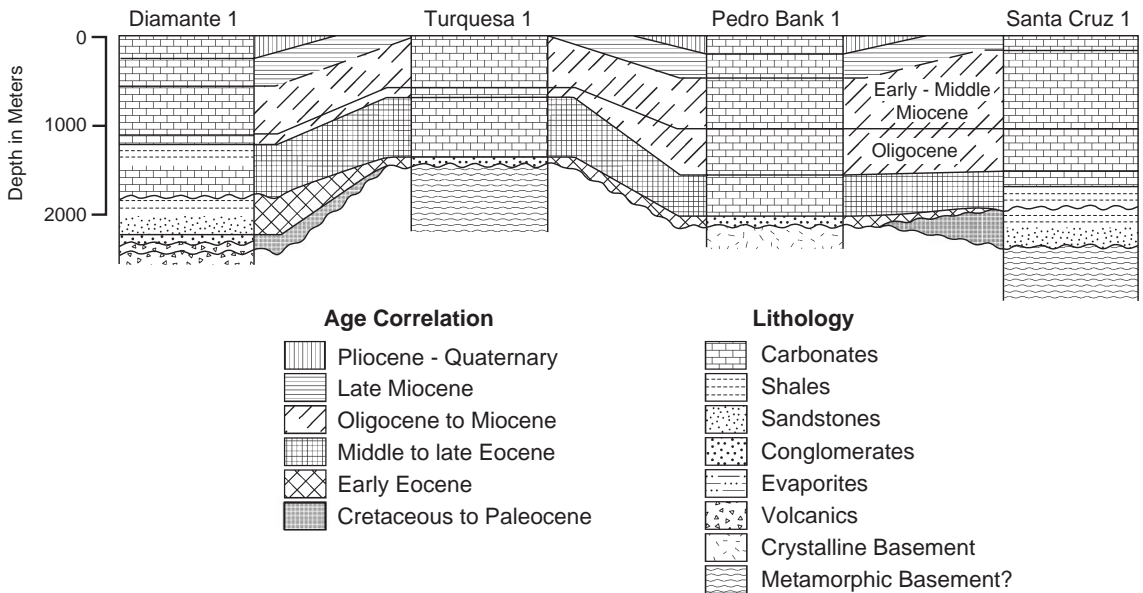


Fig. 2. Correlation among four industrial wells located in Fig. 1 (redrafted from Cunningham, 1998).

The recovery during ODP Leg 165 of sedimentary sequences of late Oligocene to middle Miocene age in present-day channels (Pedro Channel) of the NNR and north and south of the NNR (Site 998 in the Yucatan Basin and Site 999 in the Colombian Basin, respectively) (Sigurdson et al., 1997; Roth et al., 2000; Kameo and Sato, 2000), combined with information from dredged rock samples (collected During Leg II of research cruise CH9204), allows us to explore in more detail the timing and possible mechanisms for the drowning of the megabank and its relationship to Miocene climate change. In addition, we can evaluate linkages between platform drowning, climate change, and related changes in the ocean environment.

Objectives of this paper are: 1) to discuss the lines of evidence available from seismic data and dredged samples to constrain the timing of drowning; 2) to present data on sedimentological and physical properties and mass accumulation rates of slope sediments sampled at Sites 1000 and 999 by ODP Leg 165; 3) to establish a late Oligocene–Miocene stable-isotope record from bulk samples recovered at Sites 1000 and 999 as proxy of climate and circulation changes; and 4) to evaluate different hypotheses and discuss potential causes for the Miocene partial drowning of the NNR carbonate megabank.

2. Geological and oceanographic setting

The Nicaragua Rise is a major NE–SW trending active structural feature on the northwestern part of the Caribbean Plate on which carbonate platforms have been established on basement highs (Arden, 1975; Duncan et al., 1999). It is bounded by the Cayman Through to the north and by the Hess Escarpment to the south (Fig. 1). The rise is divided by the Pedro Fault Zone in the Northern and Southern Nicaragua Rise. The Northern Nicaraguan Rise (NNR) is a structural high which extends from Honduras and Nicaragua on the southwest to the island of Jamaica on the northeast, and is characterized by a series of carbonate shelves and isolated carbonate banks separated by channels and basins (Figs. 1–3). To the south is the Southern Nicaragua Rise, a deeper region of highly variable relief with rare scattered small carbonate banks, separated from the Colombian Basin by the Hess Escarpment.

The most significant oceanographic feature controlling today's sedimentation on the NNR is the northward flow of the Caribbean Current across the top of the rise and through its relatively narrow and shallow seaways (Roberts and Murray, 1983; Triffleman et al., 1992). Acceleration of the Caribbean flows over the rise induces topographic upwelling, which can raise sea-surface chlorophyll levels threefold or more with minimum temperature perturbations (Hallock and Elrod, 1988; Hallock et al., 1988). Sponge–algal communities in the photic zone dominate this upwelling, nutrient-rich environment. Because of the lower growth rate of sponge–algal communities, these platforms have failed to keep up with sea-level rise, and as a result are covered by 20–40 m of water. Because neritic carbonate production decreases rapidly with water depth, the submerged shelves and banks of the NNR were considered to be either “drowned” or “incipiently drowned” (Hine and Steinmetz, 1984). However, recent studies have shown that these carbonate shelves and banks on the NNR produce a large volume of neritic metastable carbonate sediment (fine-grained biogenic aragonite and magnesian calcite) much of which is exported offbank (Hallock et al., 1988; Droxler et al., 1991; Glaser and Droxler, 1991, 1993). Accumulation rates on the slopes during the Holocene are of the same order of magnitude as the rates off the Great Bahamas Bank (Glaser and Droxler, 1991).

3. Methodology

During a NSF-funded 1992 cruise CH9204 aboard the *R/V Cape Hatteras*, an extensive seismic grid of digital, high-resolution single channel seismic (SCS) and analog 3.5 kHz echogram data, in addition to 21 piston cores, 9 successful dredge hauls, and 2 successful box cores, was collected in Pedro Channel (see dredge locations in Fig. 3). Navigation for the SCS data consists of GPS fixes roughly every 30 shots. GPS fixes were also available for the 3.5 kHz data and at each piston core, box core, and dredge haul site. Approximately 170 km² of Hydrosweep data was acquired over ODP Site 1000, as well as over 600 km² of additional Hydrosweep data within Pedro Channel to the north of Site 1000 at the end of 1994 aboard the *R/V Maurice Ewing*. All available dredged

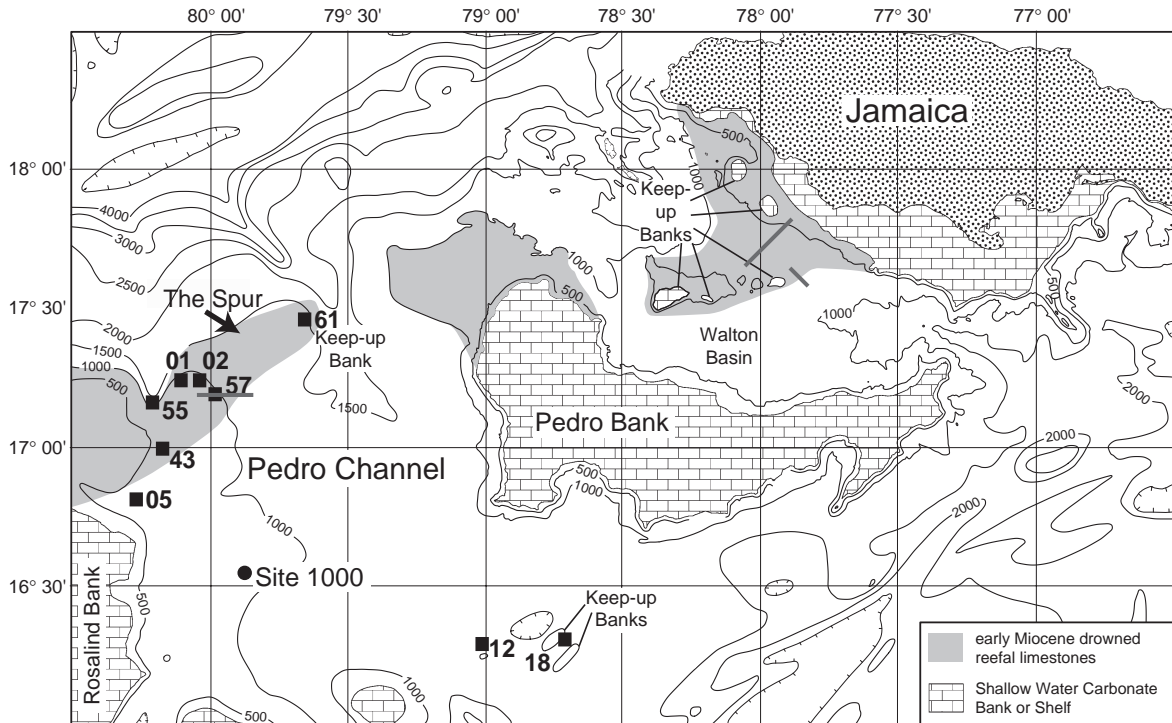


Fig. 3. Detailed bathymetric map in Pedro Channel and Walton basin (Cunningham, 1998) showing the segmented character of the seafloor within the seaways along the northern Nicaraguan Rise. The brick pattern represents present-day carbonate banks that have remained areas of neritic carbonate since the late Eocene. In grey are drowned banks and reefs observed and locally sampled (see Fig. 4). These are interpreted to have formed an east–west barrier along the northern Nicaraguan Rise where continuous shallow-water sedimentation prevailed from the Eocene to early Miocene. Note location of ODP Site 1000 in Pedro Channel. The black squares indicate location of dredge localities in Pedro Channel. The thick gray bars indicate the location of seismic lines shown in Figs. 4 and 5.

samples were cut into 2.5-cm-thick slabs for examination. Several of these slabs were then thin-sectioned to facilitate microfacies examination. Dr. Edward Robinson (University of the West Indies, Kingston, Jamaica) provided larger benthic foraminifer-based age control for several of the dredged samples (written communication). Well-lithified samples of white limestone from dredge sites CH9204-18, 57, and 61 contain larger foraminifer indicative of early Miocene (Aquitian) age. Dredge hauls CH9204-18, 43, 57, and 61 appear to have shallow-water affinities that have undergone subsequent fracturing, infilling, and diagenesis with deep-water characteristics. Planktonic infilling of cracks in some of the dredged material (sites CH9204-18 and 43) are of Pliocene or younger age. Dr. Stanley Frost (Union Oil Company) identified shallow-water Scleractinian corals in samples from dredge haul CH9204-43 (*Stylophora cf. imperatoris*)

and CH9204-57 (*Porites tronitatis* and *Montastrea costata*). Detailed description of the results and their interpretation can be found in Cunningham (1998).

ODP Leg 165 took place from December 1995 through February 1996 and cored sedimentary sequences of late Oligocene to middle Miocene age in present-day channels (Pedro Channel) of the NNR and north and south of the NNR (Site 998 in the Yucatan Basin and Site 999 in the Colombian Basin, respectively). The age models at Sites 999 and 1000 have been developed using nannoplankton and planktic foraminifers biostratigraphy (Sigurdson et al., 1997; Chaisson and D'Hondt, 2000; Kameo and Bralower, 2000) and are based on the revised geomagnetic polarity time scale of Cande and Kent (1995). Sediment mass accumulation rates (MARs; g/cm² kyr), rather than sedimentation rates (cm/kyr), were calculated for both the carbonate and non-

carbonate fractions in order to quantify the variations of the two main parameters controlling sedimentation. Mass accumulation rates are calculated by multiplying the calculated sedimentation rate (cm/kyr) by the measured dry bulk density (g/cm^3). Values from ash layers and turbidites were removed from the data set, in order to monitor “background” changes.

Over 350 samples were analyzed for bulk stable-isotope composition at both ODP Sites 999 and 1000. Bulk samples were analyzed with the intention of maintaining consistency throughout the investigated intervals, as some intervals are too lithified to be separated. Samples were dried at 60 °C, then, according to their degree of lithification, either broken and crushed or drilled to obtain sufficient material for analysis. Then they were reacted using orthophosphoric acid at 90 °C and analyzed online using a PRISM mass spectrometer at ETH Zurich. Results are reported using the standard δ notation in per mil (‰) relative to the PDB standard. Reproducibility of replicate analyses was generally better than 0.1‰. Due to different sampling intervals, the resolution of the stable isotope record is at an average of ~50 kyr (up to ~35 kyr) at Site 1000, and at an average of ~140 kyr (ranging between 80 kyr and 250 kyr) at Site 999.

4. Evolution of the Northern Nicaragua Rise

4.1. Seismic data

The speculative pre-Miocene sedimentary evolution was initiated by a marine inundation believed to have begun in the Paleocene to early Eocene. Clastic sedimentation dominated Pedro Channel until the middle Eocene when neritic carbonates were established on the banks. Based upon the interpretation of a high-resolution seismic grid and additional multi-channel seismic lines from the University of Texas Institute of Geophysics and Institut Francais du Petrole, it was concluded that a large carbonate platform, referred here to as a megabank, occupied a large portion of the NNR, in particular its crest during the Oligocene–early Miocene, including the shelves of Honduras and Nicaragua and the island of Jamaica (see Figs. 2 and 3). The current isolated carbonate platforms on the NNR such as Pedro and Rosalind

Banks were interpreted to represent the remnant parts of a partially founded megabank (Droxler et al., 1992). Moreover, the northern part of Pedro Channel, the Spur, is composed of a middle Eocene to middle Oligocene, and at least locally early Miocene remnants of a shallow-water carbonate bank. Water depths associated with the depositional environments recorded in this bank would have been close to sea level while the carbonate bank was active, compared to the 700–1200 m water depths it currently occupies. The plateau in the central part of Walton Basin is also interpreted as a drowned shallow carbonate platform and, as the Spur, is a clear drowned part of a megabank that extended across the entire crest of the NNR.

Seismic lines depict a major drowning unconformity, which separates the megabank from the overlying periplatform sediments in the northern part of Pedro Channel and in the central part of Walton Basin (Figs. 4 and 5). With the exception of the Spur in the northern part of Pedro Channel, periplatform sedimentation dominated the southern and central parts of Pedro Channel during the Neogene as recorded in ODP Site 1000.

In association with the present-day isolated carbonate banks, such as Pedro and Rosalind Banks that have remained areas of neritic carbonate since the late Eocene, drowned banks and reefs observed in Pedro Channel and Walton Basin formed an east–west barrier along the NNR, where continuous shallow-water environments prevailed from the late Eocene to early Miocene. Some of the carbonate banks and barriers subsided and drowned as late as the late early Miocene (Cunningham, 1998). The presence of these neritic banks during the early Miocene would have served as a barrier to northward water transport and would have also enhanced westward tropical flow between the Caribbean and the eastern Pacific (Fig. 3). Coccolith assemblages at Sites 998 and 999, north (Yucatan Basin) and south (Colombian Basin) of the NNR, respectively, show minimal connection in the surface circulation between those two basins during nannozones CN3 and CN4 (16.2–13.57 Ma) (Kameo and Sato, 2000). This observation supports the idea of a barrier impeding any significant surface flow over the NNR as late as during the early middle Miocene. Cunningham (1998) places the initiation of tectonic activity and mini-basin formation in the Pedro

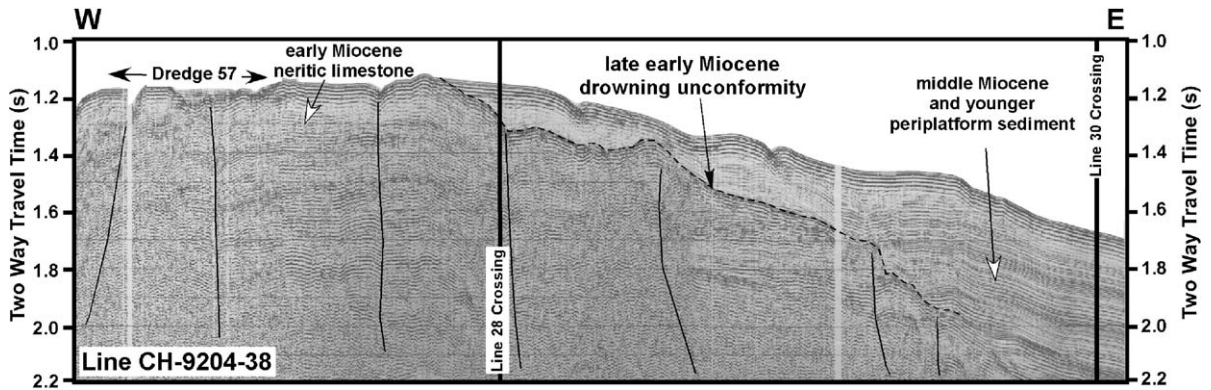


Fig. 4. Seismic line from Pedro Channel (see Fig. 3 for location) showing the seismic character of the drowned megabank and the overlying, unconformable middle Miocene and younger periplatform sediments.

Channel area at 16–11 Ma (ages of Raffi and Flores, 1995). This activity may also be related to the change from a relatively long period of quiescence on the NNR to the uplift of Jamaica in the late middle Miocene (Leroy et al., 1996). The demise of carbonate

neritic banks in the northern part of Pedro Channel and the central part of Walton Basin has led to the observed modern configuration of shallow carbonate banks segmented by north–south oriented channels (Cunningham, 1998; Droxler et al., 1998). The

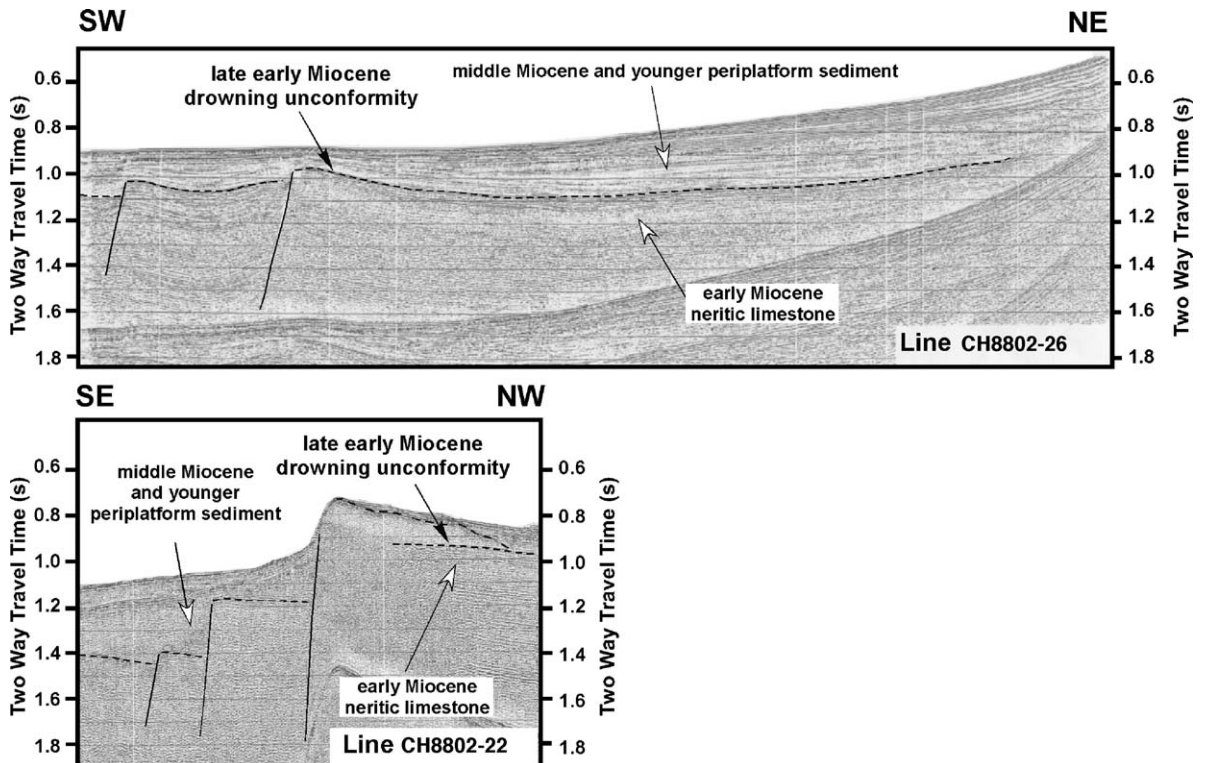


Fig. 5. Seismic lines from Walton Basin (see Fig. 3 for location) showing the seismic character of the drowned megabank and the overlying, unconformable middle Miocene and younger periplatform sediments.

merging of coccolith assemblages between Sites 998 and 999 (Kameo and Sato, 2000) was first initiated during nannozone CN5 (13.57–10.71 Ma) and was fully completed during nannozones CN6 and CN7 (10.71–9.36 Ma) and supports the estimated timing of a seaway opening along the NNR.

4.2. Dredge samples

Although the top of the drowned megabank was never cored, the top of the foundered megabank or its lateral, deeper-water equivalent crops out on the seafloor in several locations within Pedro Channel (Cunningham, 1998). During the research cruise

CH9204, nine successful dredge hauls were collected in Pedro Channel (see Fig. 3 for location). Petrographic analyses of dredged samples have revealed the presence of shallow-water organisms (see Fig. 6) such as corals, green algae, and larger benthic foraminifers, mixed with pelagic organisms. Shallow-water components have been redeposited in deeper water either as single components or as part of larger, lithified clasts (Cunningham, 1998). This is especially evident in samples from site CH9204-57 where there are clasts consisting exclusively of layered shallow-water sands that are incorporated into a mix of shallow-water and pelagic material. The shallow benthic biota, as discussed below, gives an

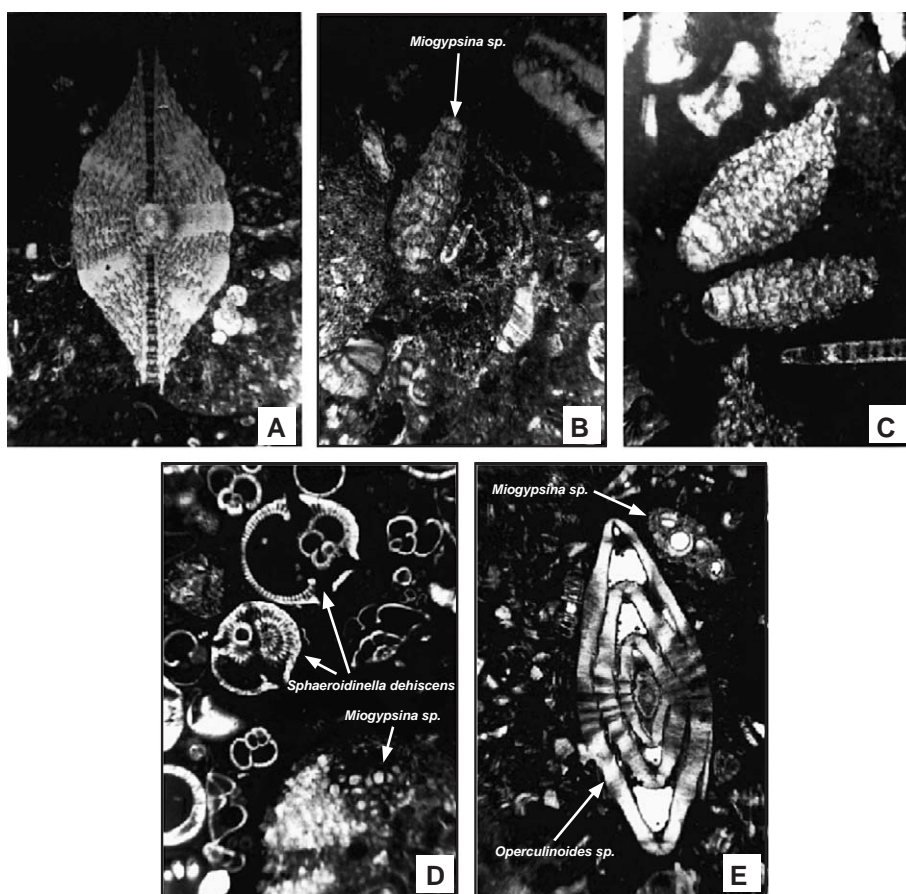


Fig. 6. Photomicrographs of biogenic components occurring in the dredge samples. (A and B) Sample from Site CH9204-61 illustrating *Lepidocyclina giraudi* (larger foraminifers) (A) and *Miogypsina* sp. (probably *Miogypsina gunteri*) (B); (C) sample from dredge site CH9204-18 illustrating *Miogypsina* sp. larger benthic foraminifers; (D) sample from dredge site CH9204-18 illustrating *Miogypsina* sp. and *Sphaeroidinella dehiscens*; (E) sample from site CH9204-57 illustrating *Operculinoides* sp. and *Miogypsina* sp. larger benthic foraminifers. All photomicrographs and foraminifer identification are courtesy of Dr. E. Robinson.

early Miocene minimum age for the shallow-water limestones (20–22 Ma; Cole, 1967; Bryan and Huddleston, 1991; Robinson, 1994). Well-lithified samples of white limestone from dredge sites CH9204-18, 57, and 61 contain larger foraminifer indicative of early Miocene (Aquitanian) age. Dredge hauls CH9204-18, 43, 57, and 61 appear to have shallow-water affinities that have undergone subsequent fracturing, infilling, and diagenesis with deep-water characteristics. Planktonic infilling of cracks in some of the dredged material (sites CH9204-18 and 43) is of Pliocene or younger age. Larger benthic foraminifers at site CH9204-18 include *Lepidocyclina* (*Lepidocyclina*) *giraudi* and *Miogypsina* sp. (Fig. 6), indicating an early Miocene, Aquitanian age for the sample. Shallow-water Scleractinian corals were identified in samples from dredge haul CH9204-43 (*S. cf. imperatoris*) and CH9204-57 (*P. tronitatis* and *M. costata*).

The available data set does allow to discriminate whether this deeper environment represents the fore-reef (10–30 m water depth) or deeper slope environments (see discussion in Cunningham, 1998). The depositional environment interpretation based on the analysis of dredged samples would thus indicate that periplatform sedimentation has dominated Pedro Channel from the early Miocene to recent. Southeast Pedro Channel (see Fig. 3) appears to be a faulted half-graben that was tectonically active from 25 to 21 Ma and from 16 to 8 Ma. The Spur (see Fig. 3) is interpreted as a drowned carbonate bank, which partially drowned in the late Oligocene around 27 Ma and gave up in the late early Miocene after 20 Ma, resulting in no further neritic coral growth. The speculative pre-Miocene sedimentary evolution reflects a marine inundation believed to have begun in the Paleocene to early Eocene. Clastic sedimentation dominated Pedro Channel until the middle Eocene when neritic carbonates were established on the banks.

5. ODP sites

Data from two ODP sites will be discussed, from the shallower Site 1000, currently at 927.2 m water depth, to the deeper Site 999, currently at 2838.9 m water depth (see Fig. 1).

5.1. Site 1000

Site 1000 was drilled in Pedro Channel, the largest (150 km wide) channel crossing the NNR, which is flanked by Pedro Bank to the east and Rosalind bank to the west (Figs. 1 and 3). The section drilled at Site 1000 comprises a continuous, fairly homogeneous lower Miocene–recent 696-m-thick section, which consists dominantly of periplatform sediments and sedimentary rocks, interbedded with volcanic ash layers and intervals of redeposited pelagic and neritic carbonates from the adjacent shallow carbonate banks (Sigurdson et al., 1997).

The interval investigated at Site 1000 ranges from 370 to 696 m (the bottom of the recovered section), spanning from the early Miocene (the oldest rocks recovered at this site) through the base of the late Miocene (Fig. 7). This interval comprises different lithological units (Units IC, ID, IIA, and IIB; see Fig. 7) determined ship-board on the basis of sedimentologic criteria, magnetic susceptibility, color reflectance, and carbonate content (Sigurdson et al., 1997). Periplatform pelagic carbonates form the background sediment, and are interspersed with volcanic ash layers and bank-derived calcareous turbidite layers.

Volcanic ash layers are most abundant in the lower part of the cored section (early Miocene to early middle Miocene). A similar peak in volcanism was also recognized at Sites 998 and 999 (Sigurdson et al., 1997; Carey and Sigurdson, 2000). The occurrence and distribution of volcanic ash layers document a major episode of volcanism in the western and central Caribbean beginning in the earliest Miocene (20–22 Ma) and extending through the middle Miocene, with ashes accumulation rates ranging up to 2 m/myr (Sigurdson et al., 1997).

The calcareous turbidites show distinctive changes in distribution downcore (Fig. 8). On the basis of turbidite abundance, three intervals can be defined. Two intervals characterized by a high frequency of turbidites are identified. The first interval occurs from 696 to 585 m and coincides with lithological Unit IIB, whereas the second interval occurs within Unit IC, between 405 and 300 m. A third interval, between 585 to 405 m, spanning the middle Miocene, is turbidite-free, with the exception of one single bed (Fig. 8). Most of the turbidites contain redeposited pelagic components, and only the lowermost turbidite beds

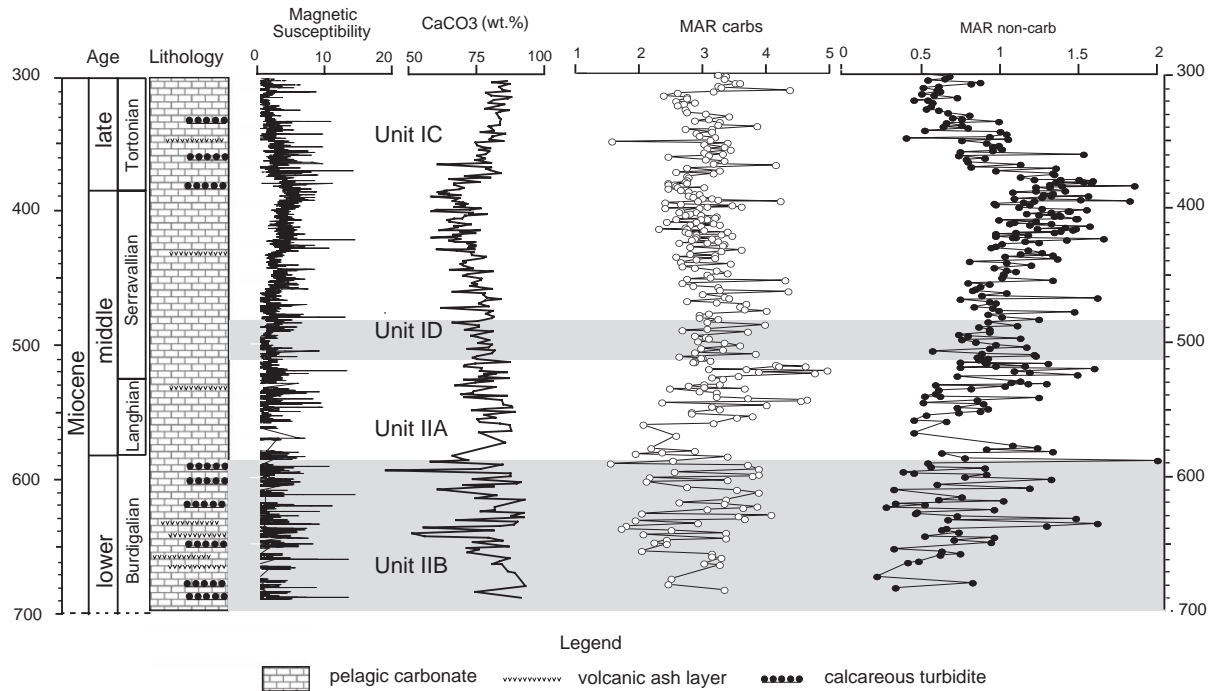


Fig. 7. Lithological units in the investigated interval at Site 1000 (Units IC, ID, IIA, and IIB) reflect primarily changes in magnetic susceptibility, carbonate content, and degree of lithification (modified from Sigurdson et al., 1997; Mutti, 2000). Note the occurrence of volcanic ash layers and calcareous turbidites within the pelagic sediments. Mass accumulation rates (MARs) have been calculated for the carbonate and the non-carbonate fraction. MARs were obtained by combining carbonate/non-carbonate contents and age model with density measurements made during Leg 165 (Sigurdson et al., 1997).

contain material derived from the shallow-water portion of the adjacent banks, such as benthic foraminifers. These turbidites that contain platform-derived material suggest that the adjacent banks were still active during the Burdigalian, in agreement with information obtained from dredged samples.

At Site 1000, MARs for both the carbonate and non-carbonate fraction show marked variations throughout the investigated section (Fig. 7). Carbonate MARs are generally high (3–10 times the non-carbonate fraction) and show the highest values in the Langhian. Non-carbonate MARs show a systematic increase from the base of the cored interval throughout the Serravallian, with peaks in the Burdigalian, Langhian, and Serravallian.

5.2. Site 999

Site 999 is located on the Kogi Rise, approximately 1000 m above the turbidite-laden floor of the

Colombian Basin (Fig. 1). A 1066.4-m-thick continuous and apparently complete upper Maastrichtian–Pleistocene section was recovered, and consists dominantly of pelagic sediments and sedimentary rocks with variable amounts of clays and volcanic ash. The investigated interval at Site 999 ranges from 580 to 250 m, spanning from the Oligocene/Miocene boundary through the base of the late Miocene (Fig. 9). This interval comprises different lithological units (Units IIA and IIB, and Unit III; see Fig. 9) determined by ship-board observations on the basis of sedimentologic criteria, magnetic susceptibility, color reflectance, and carbonate content (Sigurdson et al., 1997). Volcanic ash layers are particularly abundant in the lower Miocene to lower middle Miocene portion of the section. The volcanic ash sedimentation rate at this site is higher by about one order of magnitude with respect to Sites 999 and 1000, suggesting that the Colombian basin was closer to the principal fall out of the Miocene volcanic source.

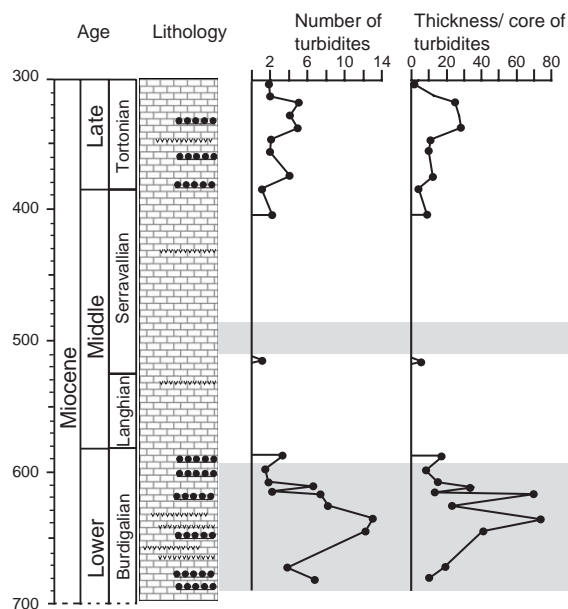


Fig. 8. Turbidites at Site 1000. The grey bars refer to the lithological units illustrated in Fig. 7 (legend as in Fig. 7).

MARs of the carbonate fraction at Site 999 increase abruptly in the middle Burdigalian, and this high accumulation rate persists through the Langhian (Fig. 9). The MARs of the non-carbonate fraction also show an increase during the same time interval, although less marked. The abruptness of this change may be an artifact of the age model, but not the relative changes in values.

6. Significance of variations in turbidite abundance and MARs

The high-carbonate MARs at Site 1000 (see Fig. 7) generally indicate the proximity to a periplatform environment, where pelagic settling is mixed with other fine sediments derived from the surrounding banks. Turbidites are particularly abundant during the Burdigalian and again in the Tortonian. Most of the turbidite beds we examined in thin section are composed of reworked and sorted planktic foraminifers, but some larger benthic foraminifers occur in the lowermost part of the cored interval. The highest values in carbonate MARs are observed during the Langhian, out of phase with turbidite occurrence. This could be

interpreted to reflect increased pelagic input at this time and would also be consistent with an increase in primary productivity. This is particularly evident at Site 999, where most of the sediment is derived from pelagic settlings, and high carbonate MARs strongly suggest a regional increase in primary productivity. Non-carbonate MARs at Site 1000 show a systematic increase from the base of the cored interval throughout the Serravallian, with peaks in the Burdigalian, Langhian, and Serravallian. At Site 999, MARs for the carbonate and non-carbonate fraction covary from the middle Burdigalian through the Langhian, but this trend is reversed at the Langhian/Serravallian boundary. This change suggests that the two parameters reflect a response to independent forcing factors.

7. Stable isotope data

7.1. Site 1000

The oxygen-isotope record from bulk sediment at Site 1000 (Fig. 10) shows marked variations, ranging from -2.7‰ to -0.3‰ , with a systematic trend towards heavier values upsection, and shows the detailed character of middle Miocene events. Three major first-order features are present: 1) an interval with high variability but without a marked trend during the Burdigalian (lithological Unit IIB); 2) a phase of progressive shift towards higher values, from 2.3‰ to -0.9‰ , peaking at -0.3 , which records the mid Miocene $\delta^{18}\text{O}$ increase (lithological Unit IIA); and 3) relatively constant values during the Serravallian (lithological Units ID and IC), with values ranging from -1.7‰ to -0.6‰ .

The carbon-isotope record (Fig. 10) shows marked variations, from 0.5‰ to 2.2‰ , with one major positive excursion. The $\delta^{13}\text{C}$ shift towards higher values occurs stepwise, initiating during the Burdigalian, with a gradual increase from 0.9‰ to 1.5‰ , then rapidly increasing to 2.2‰ at the end of the Burdigalian (lithological Unit IIB), remaining high during the Langhian (lithological Unit IIA). The $\delta^{13}\text{C}$ values start returning gradually to lower values throughout the Serravallian (lithological Unit ID), reaching 0.7‰ , returning to higher values up to 1.6‰ , and the excursion terminates with an abrupt decrease from 1.6‰ to 0.6‰ at the end of the Serravallian.

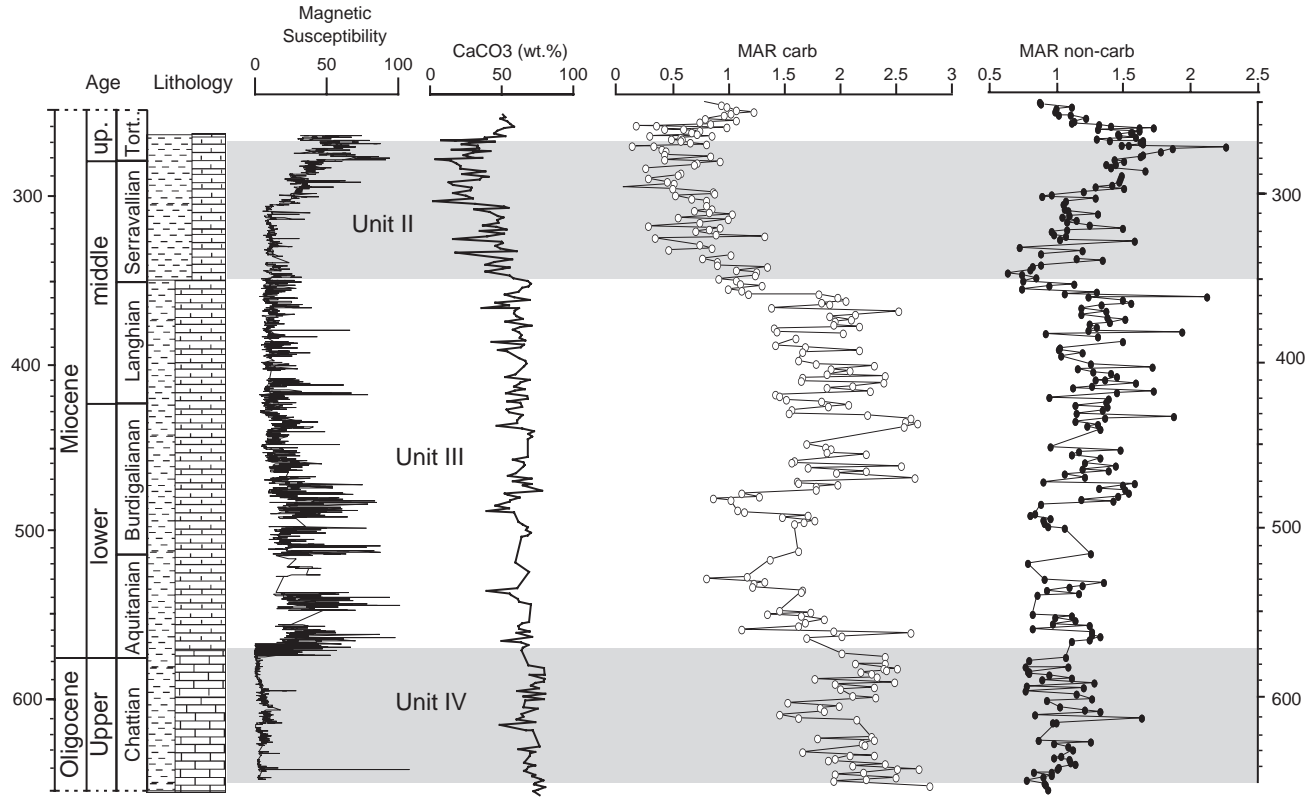


Fig. 9. Lithological units in the investigated interval at Site 999 (Units IC, IIA, and IIB, Unit III, and Unit IVA) reflect primarily changes in magnetic susceptibility, carbonate content, and degree of lithification (modified from Sigurdson et al., 1997; Mutti, 2000). MARs have been calculated for the carbonate and the non-carbonate fractions by combining carbonate/non-carbonate contents and age models with density measurements made during Leg 165 (Sigurdson et al., 1997).

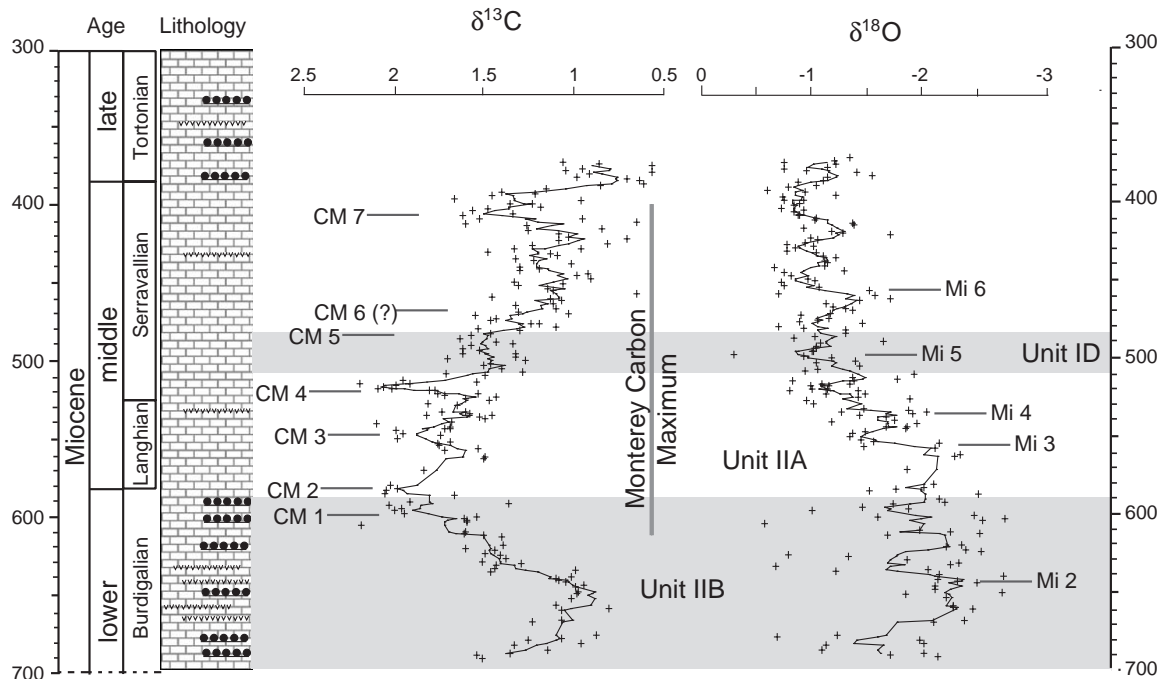


Fig. 10. Carbon- and oxygen-isotope data from Site 1000, plotted against depth. The grey bars refer to the lithological units as illustrated in Fig. 7. Values are in per mil (‰). The crosses indicate actual measurements; the black line indicates the same data smoothed with a five-point running average. Note that this removes periods shorter than ~300 kyr. The inflections in $\delta^{18}\text{O}$ reveal the presence of isotope events Mi2, Mi3, Mi4, and Mi5 (as defined by Miller et al., 1996, 1998; Wright et al., 1992). Carbon isotope events CM1, CM2, CM3, CM4, CM5, and CM7 (as defined by Woodruff and Savin (1989) reveal the structure of the Monterey Carbon Isotope Excursion (Vincent and Berger, 1985).

7.2. Site 999

The oxygen-isotope record shows marked variations, ranging from -2.6‰ to -0.3‰ (Fig. 11). Oxygen-isotope values show: 1) an interval of intermediate variability, with an overall trend towards lighter values during the Chattian and Aquitanian (lithological Unit IV and part of Unit III); 2) a phase of relatively constant values throughout the Burdigalian and Langhian (middle and upper part of Unit III); and 3) an increase at the boundary between lithological Units III and II, from -1.3‰ to -0.5‰ .

The carbon-isotope record shows marked variations, from 0.5‰ to 2.4‰ , and also includes the presence of two positive excursions (Fig. 11). The first positive excursion occurs at the top of lithological Unit IV, near the Oligocene–Miocene boundary. The second and major positive excursion in $\delta^{13}\text{C}$ occurs within lithologic Unit III and is a gradual, stepwise increase, occurring over several tens of meters. The

shift initiated in the late Burdigalian, from 0.9‰ to 1.8‰ , returning to 1.3‰ and then rapidly increasing to 2.4‰ during the Langhian. The carbon values remain high for an interval of approximately 40 m, and then start returning gradually to lower values throughout the Serravallian (lithological Unit II). The excursion terminates with a return to $\sim 1\text{‰}$ at the end of the Serravallian.

7.3. Chemostratigraphic significance of isotope records

When comparing the data set generated at Sites 999 and 1000 with other existing records (e.g., Miller et al., 1998; Zachos et al., 2001), a major difference to consider is that data generated in this study reflect bulk rock analysis, rather than measurements on specific species of foraminifers, as commonly used in Cenozoic paleoceanographic studies. Bulk rock analysis is, however, commonly used in many pre-

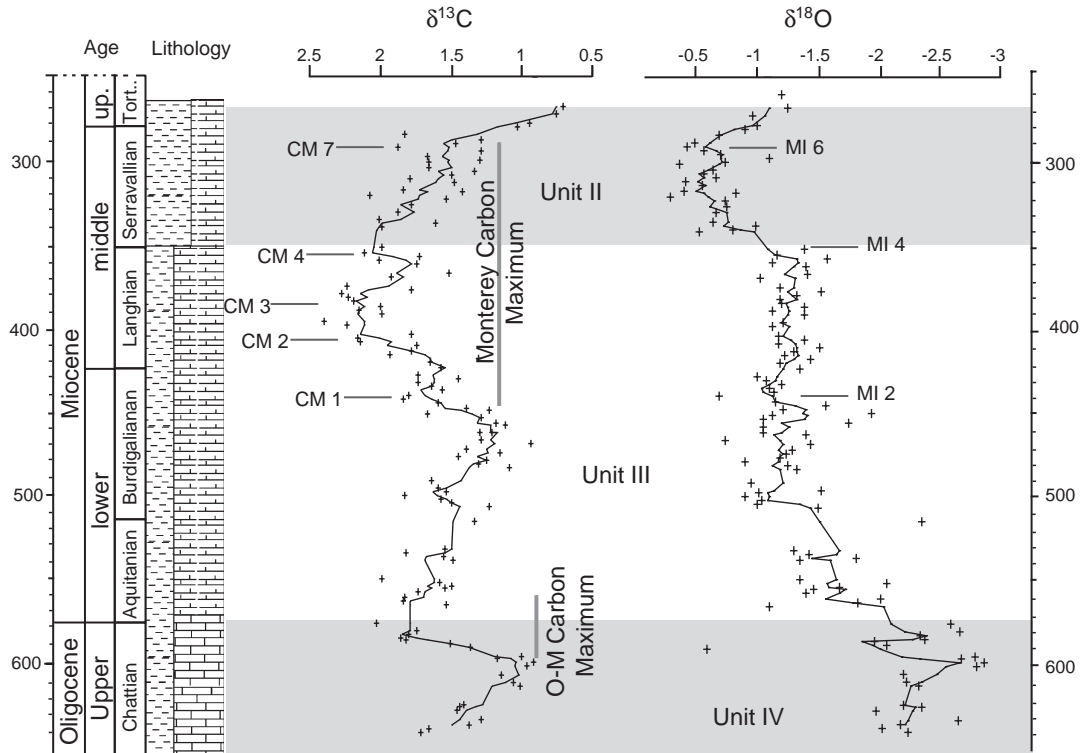


Fig. 11. Carbon- and oxygen-isotope data from Site 999, plotted against depth. The grey bars refer to the lithological units as illustrated in Fig. 9. Values are in per mil (‰). The crosses indicate the actual measurements; the black line indicates the same data smoothed with a five-point running average. Note that this removes periods shorter than ~300 kyr. Due to the lower sampling resolution with respect to Site 1000, only oxygen-isotope events Mi2, Mi4, and Mi6 (as defined by Wright et al., 1992; Miller et al., 1996, 1998) can be recognized. Note the two major carbon isotope excursions: the first is the Oligocene–Miocene boundary (Zachos et al., 1997) and the second is the Monterey Carbon Isotope Excursion (Vincent and Berger, 1985), and the presence of carbon isotope events CM1, CM2, CM3, CM4, and CM7 (as defined by Woodruff and Savin, 1989).

Cenozoic pelagic settings, when lithologies are usually too lithified to allow separation of foraminifer species. Even though bulk analyses reflect a mixing of carbonates from different sources, it has been shown that under certain circumstances, the isotopic composition derived from bulk analyses resembles closely the record derived from single foraminifer analyses (Shackleton et al., 1993).

The isotopic composition of bulk samples analyzed in this study reflects primarily the composition of calcareous nannoplankton and planktic foraminifers, with minor contributions from benthic foraminifers. This implies that isotope values will reflect primarily surface conditions and will be characterized by higher isotope values with respect to deep sea benthic foraminifer records (Miller et al., 1998; Zachos et al., 2001).

A second aspect to consider is regarding the possibility of post-depositional diagenetic alteration that can modify the original marine values, especially the oxygen isotopes. Frank et al. (1999) have shown that with increasing CaCO_3 content and burial depth, bulk rock values show progressively lower $\delta^{18}\text{O}$ values. Using CaCO_3 content as a proxy to evaluate the extent of diagenetic modification, Mutti (2000) has shown that the $\delta^{18}\text{O}$ values above 570 mbsf at Site 999, and above 590 mbsf at Site 1000, can be assumed to reflect primary values and can therefore be used for paleoceanographic purposes.

At Site 1000 (see Fig. 10), the inflections in the $\delta^{18}\text{O}$ reveal the presence of the Miocene oxygen-isotope events Mi2, Mi3, Mi4, and Mi5 (as defined by Miller et al., 1996, 1998; Wright et al., 1992) and

shows the detailed structure of the middle Miocene $\delta^{18}\text{O}$ increase; this, totaling 1.4‰, occurs within several (three to four) quasi-cyclic steps. Due to the lower sampling resolution used at Site 999 (see Fig. 11), only oxygen-isotope events Mi2, Mi4, and Mi6 are visible (as defined by Miller et al., 1998).

The marked variability of carbon isotopes reveals at Site 1000 (see Fig. 10) the presence of high $\delta^{13}\text{C}$ values between ~17 and 13.5 Ma, well known as the Monterey Carbon Isotope Excursion (Vincent and Berger, 1985). Furthermore, it is possible to recognize the detailed structure within this event, expressed by carbon isotope events CM1, CM2, CM3, CM4, CM5, and CM7 (as defined by Woodruff and Savin, 1989). The Monterey Carbon Isotope Excursion is also clearly visible at Site 999 (see Fig. 11), as well as

carbon isotope events CM1, CM2, CM3, CM4, and CM7. Furthermore, at Site 999, the $\delta^{13}\text{C}$ increase near the Oligocene–Miocene boundary is visible (Zachos et al., 1997, 2001).

The chemostratigraphic events in the oxygen and carbon-isotopes records recognized in the Site 999 and 1000 records can be well traced between the two sites (Figs. 12 and 13). The correlation between the two sites further confirms that the stable isotope events recognized are representative of primary marine values. Variations in stable isotopes from both Sites 999 and 1000 indicate regional changes in climate and circulation during the late Oligocene–middle Miocene and are linked to major changes in climate associated with the transition from relative global warmth to the Neogene “ice-house” world.

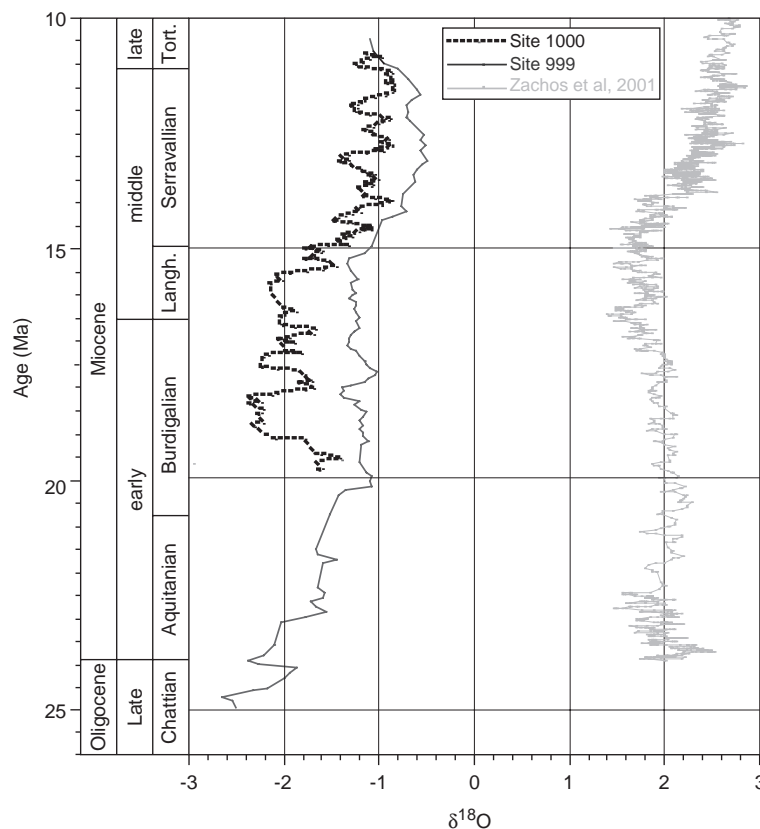


Fig. 12. The oxygen-isotope record from Sites 999 and 1000, plotted against time (rather than against as depth, as done for Figs. 7–9) to facilitate comparison among the two sites and with the deep-sea record compiled by Zachos et al. (2001). Note how the $\delta^{18}\text{O}$ record at Sites 999 and 1000 clearly indicates the middle Miocene $\delta^{18}\text{O}$ increase from ~15.5 to 13 Ma, although the values are 3–4‰ higher with respect to deep-sea benthic foraminifer records (see Zachos et al., 2001).

8. Paleoenvironmental significance of isotope data

8.1. Oxygen isotopes

A number of features emerge from a comparison of the $\delta^{18}\text{O}$ record from Sites 999 and 1000 with globally recognized Miocene oxygen-isotope events (as defined by Wright et al., 1992; Miller et al., 1996, 1998; Zachos et al., 2001). The inflections in the $\delta^{18}\text{O}$ record at Sites 999 and 1000 indicate clearly the middle Miocene $\delta^{18}\text{O}$ increase from ~15.5 to 13 Ma (Fig. 12), although the values are 3–4‰ higher with respect to deep-sea benthic foraminifer records (see Zachos et al., 2001). The middle Miocene $\delta^{18}\text{O}$ increase has been interpreted to primarily record the

intensification of continental glaciation in Antarctica (Savin et al., 1975; Savin and Woodruff, 1990; Shackleton and Kennett, 1975). In this interpretation, cooling of high southern latitude surface waters increased the production of deep and intermediate waters and enhanced vertical stratification throughout the world ocean. A different interpretation suggests that large ice sheets may have existed prior to the middle Miocene and that the middle Miocene $\delta^{18}\text{O}$ increase was entirely due to deepwater cooling, unaccompanied by Antarctic ice growth (Matthews and Poore, 1980; Prentice and Matthews, 1988). The relative proportions of $\delta^{18}\text{O}$ increase attributable to Antarctic ice storage or to bottom water cooling remain uncertain.

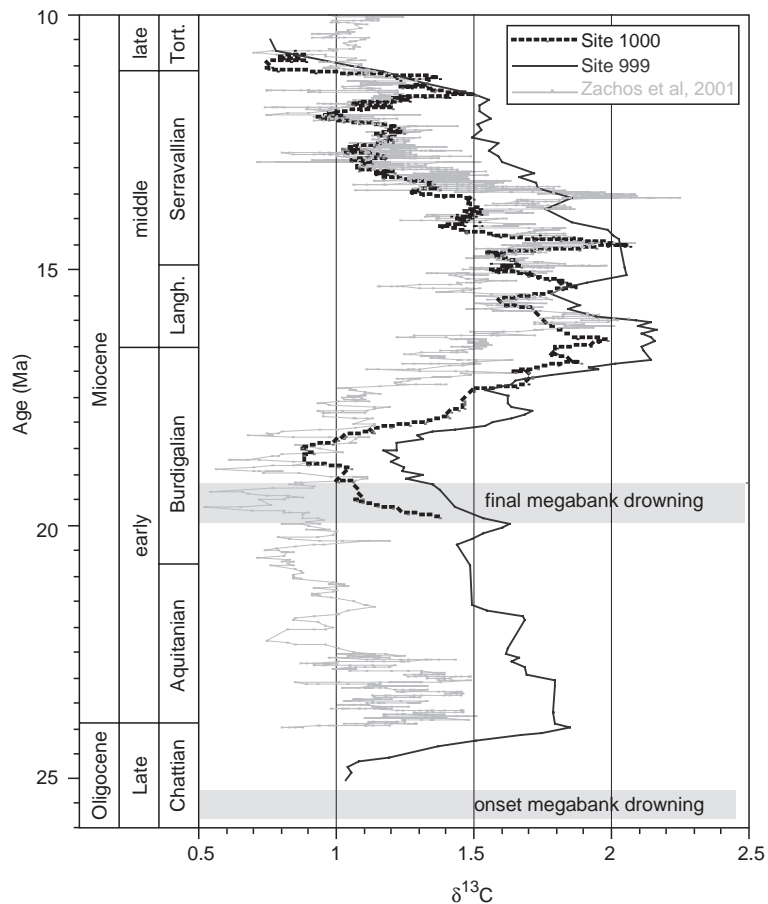


Fig. 13. The carbon-isotope record from Sites 999 and 1000, plotted against time (rather than against as depth, as done for Figs. 7–9) to facilitate comparison among the two sites and with the deep-sea record compiled by Zachos et al. (2001). The grey bars indicate the timing of the drowning events.

For the purpose of this paper, it is important to notice that the drowning episodes, starting in the late Oligocene and culminating in the Burdigalian, clearly predate the most significant middle Miocene $\delta^{18}\text{O}$ increase. The Site 1000 record (Fig. 10) indicates how Burdigalian drowning episode predates isotope event Mi2.

8.2. Carbon isotopes

A comparison of the $\delta^{13}\text{C}$ record from Sites 999 and 1000 with globally recognized carbon-isotope trends and events (Fig. 13) indicates the presence of two major maxima in mean ocean $\delta^{13}\text{C}$: the first (Site 999 only) near the Oligocene–Miocene boundary, around 24 Ma (Zachos et al., 1997, 2001), and the second (both Sites 999 and 1000) during the late early to middle Miocene, from 17 to 13.5 Ma (Monterey Carbon Isotope Excursion; Vincent and Berger, 1985).

Miocene paleoceanographic changes were accompanied by major variations in mean ocean $\delta^{13}\text{C}$, involving redistribution between carbon reservoirs (Miller and Fairbanks, 1985; Vincent and Berger, 1985). The Monterey $\delta^{13}\text{C}$ maximum has been attributed to the storage of large volumes of organic carbon in the Monterey Formation of California, circum-North Pacific, and the southeastern shelf of the United States, and is postulated as a major contributor to global cooling through drawdown of atmospheric CO_2 and a series of positive feedback mechanisms (Vincent and Berger, 1985). The Miocene was a time of unusually high accumulation of organic matter around the Pacific (e.g., Monterey Formation, California; Ingle, 1981; Vincent and Berger, 1985), Atlantic (Florida shelf; Compton et al., 1990), and Mediterranean (Tellaro Formation, Sicily; Mutti et al., 1999). Woodruff and Savin (1989) suggested that the seven $\delta^{13}\text{C}$ maxima (CM events) found within the Monterey Carbon Isotopic Excursion correspond to episodes of accumulation of especially large amounts of organic matter around the world.

The drowning episodes, starting in the late Oligocene and culminating in the Burdigalian around 20 Ma, predate the onset of the two main carbon maxima, each by approximately 1–2 myr. This relationship between drowning and onset of positive excursions in $\delta^{13}\text{C}$ is similar to those of Mutti et al.

(1997), who have been recognized in the central Mediterranean.

9. Discussion of drowning mechanisms

9.1. Timing of drowning events and subsidence pulses

Droxler et al. (1998) originally suggested that the foundering of the NNR megabank was possibly related to a reorganization of the spreading within the Cayman Trough. However, the integration of regional seismics with dredge data has revealed pulsed subsidence changes (Cunningham, 1998) with two major phases: one at 21–25 Ma and the second at 16–8 Ma (see Fig. 14). Because the major drowning phases are not coincident in time with these events, an environmental mechanism must have been acting on the longer term to reduce the growth potential of the NNR carbonate platforms. Schlager (1999) has demonstrated that the growth potential of carbonate platforms follows a scaling trend, providing a solution to the drowning paradox (Schlager, 1981, 1999; Hallock and Schlager, 1986). The long-term (millions of years) drowning of carbonate platforms requires that the reduction of growth with increasing time is largely caused by environmental factors. Several processes could have resulted in long-term local environmental changes: increased volcanic activity; changes in circulation that would result in increased local productivity of the surface waters; and changes in sealevel and temperature of the surface waters.

9.2. Increased volcanic activity

Major volcanic eruptions such as those documented in the Caribbean during the Miocene are expected to have a strong negative effect on carbonate growth rates. Volcanic events would have increased water turbidity, thus reducing light penetration to the surface ocean. Calculated accumulation rates of ash layers indicate a peak (up to 2 m/myr) during the early Miocene (Sigurdson et al., 1997). This would have likely resulted in increased water turbidity at that time. Non-carbonate MARS, however, do not show significant variability coincident in time with the drowning episodes (Fig. 14). We suggest that frequent and intense volcanic eruptions may have provided an

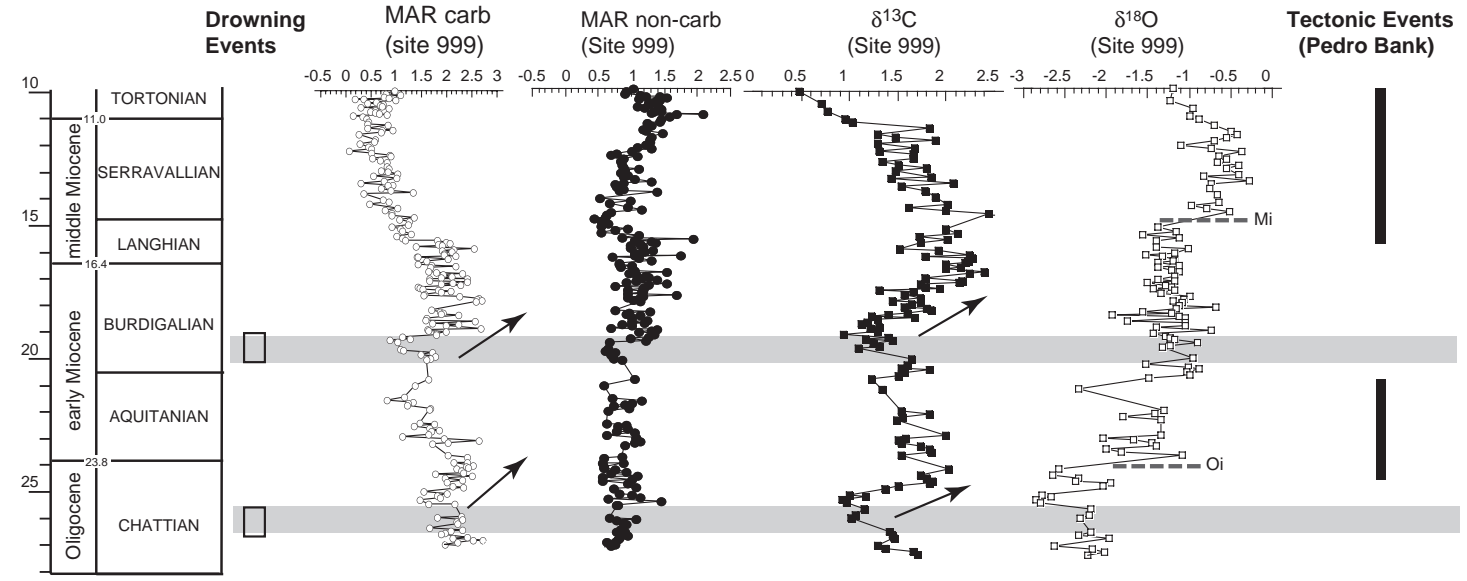


Fig. 14. Summary of the model proposed to explain changes in neritic carbonate production and export on the Nicaraguan Rise. Tectonic events are from Cunningham (1998).

overall higher turbidity with respect to “normal” values, but they alone cannot be responsible for the drowning of the banks.

9.3. Changes in temperature of the surface waters

Temperature changes and sealevel changes are linked to glacioeustasy. Times of inflections in the $\delta^{18}\text{O}$ defining the oxygen-isotope events discussed above correspond to sea-level falls (Miller et al., 1996, 1998). Given the uncertainty in the relative contribution of cooling versus ice storage, the amplitudes of the sea-level falls remain debated (e.g., John et al., 2004). The relative timing of drowning with respect to the oxygen-isotope events would exclude the role of temperature changes in the drowning. Furthermore, because the sites are located in the tropical ocean, variations in sea-surface temperature related to oxygen-isotope events are expected to be minor and are therefore unlikely to be responsible for platform drowning. The Burdigalian drowning episode occurs immediately before isotope event Mi2 (see Site 1000 record; Fig. 10), which corresponds to a sea-level fall related to ice growth, thus suggesting that drowning corresponds to a time of higher sea level.

9.4. Changes in nutrient supply to surface waters

The two main drowning events in the NNR occur at the onset of increases in MAR of pelagic carbonate, which is a direct reflection of increases in productivity in the surface waters (Fig. 14). These MAR increases predate by approximately 1 myr the onset of positive excursions in $\delta^{13}\text{C}$, both in the late Oligocene and in the late early Miocene, at the onset of the Monterey Carbon isotope excursion.

Studies on Caribbean corals are consistent with regional changes in productivity. About half of the Caribbean hermatypic corals became extinct during the latest Oligocene and the early Miocene (Frost, 1977; Budd, 1990; Edinger and Risk, 1994). Of these, the majority were geographically restricted to the Indo-Pacific, the remainder became globally extinct (Frost, 1977). Paleontological studies (Edinger and Risk, 1994) on land sections suggest evidence of a major ecological crisis at the Oligo-Miocene boundary, with survival of those coral

tolerant of both turbidity and high nutrients. Extensive phosphorite deposits, typically associated with enhanced upwelling, were formed throughout the Caribbean during the early Miocene (Edinger and Risk, 1994).

The timing of drowning seems to coincide with regional changes in productivity and upwelling, as suggested by MAR at Sites 999 and 1000, coral extinction patterns, and concurrent regional occurrence of phosphorites. Hallock and Elrod (1988) suggested that nutrient increases due to topographic upwelling have major effects on today's sedimentation. This scenario could be used to explain the drowning of the megabank during the late Oligocene and the Burdigalian by nutrification.

9.5. Possible causes for changes in nutrient supply

What could provide a mechanism to increase nutrient supply and upwelling to the Caribbean in the late Oligocene–early Miocene and an explanation for the relationships observed? The equatorial Pacific is today one of the zones characterized by the highest productivity and was also during the Miocene. Paleolatitude reconstructions of the Caribbean for the early to middle Miocene suggest that the NNR was then located at a latitude similar to the present (Acton et al., 2000). The paleogeographic setting, however, had important differences. The connection between the east Pacific and the Caribbean across the open Central American Seaway in the late Oligocene and early Miocene is a likely explanation for the high trophic conditions. Because of this paleogeographic configuration, the megabank was exposed to abnormally high nutrient levels associated with Miocene equatorial productivity. Wilson et al. (1988) have proposed the “Death-in-the-Tropics” hypothesis, showing that Cretaceous guyots drowned sequentially over a wide range of time while they were being transported northward by motion of the Pacific plate (through a narrow paleolatitudinal zone $\sim 0\text{--}10^\circ\text{S}$). The paleogeographic setting of the NNR during the late Oligocene and early Miocene was overall consistent to high nutrient supplies. However, the specific mechanisms that intensified nutrient supply in correspondence to the drowning phases remain unclear.

9.6. Drowning of the megabank and initiation of the Caribbean Current

The foundering of the megabank led to the opening of a major intra-Caribbean gateway (Droxler et al., 1998). Since its formation, Pedro Channel has been a major pathway for the Caribbean Current and, therefore, for the surface and thermohaline return flow of the modern thermohaline circulation. The merging of coccolith assemblages between Sites 998 and 999 (Kameo and Sato, 2000) was first initiated during nannozone CN5 (13.57–10.71 Ma) and was fully completed during nannozones CN6 and CN7 (10.71–9.36 Ma) and supports the estimated timing of a seaway opening along the NNR. The foundering of the NNR megabank is consistent with an overall strengthening of the Western Boundary Current (Caribbean Current, Loop/Florida Current, and Gulf Stream) in middle Miocene times, as recorded by middle Miocene erosional events on the central West Florida shelf (Mullins and Neumann, 1979; Mullins et al., 1987), the Straits of Florida (Gomberg, 1974; Mullins and Neumann, 1979), and the Blake Plateau (Popenoe, 1985).

10. Conclusions

(1) The modern system of banks, seaways, and basins on top of the NNR has evolved from a continuous, shallow-water carbonate megabank that extended from the Honduras/Nicaraguan mainland to Jamaica. Available information suggests that this megabank broke apart and partially drowned in the late middle Oligocene around 27 Ma. Individual banks foundered until the late early Miocene after 20 Ma, resulting in no further neritic coral growth.

(2) Stratigraphic units identified in deep-water carbonates sampled at ODP Sites 999 and 1000 help to constrain the environmental setting leading to the drowning of the banks. Changes in lithology and mass accumulation rates of both the carbonate and non-carbonate fractions parallel stable-isotope shifts indicative of regional changes in climate and circulation during the late Oligocene–middle Miocene.

(3) Carbonate accumulation at Site 999 suggests increased regional productivity during the early Miocene. Terrigenous accumulation at both Sites

999 and 1000 indicates a general increase from the Burdigalian through the Serravallian. The temporal association among episodes of platform growth, followed by increased productivity as identified by higher carbonate MARs and positive excursion in carbon isotopes, all suggest that nutrification changes have led to the drowning of the NNR “megabank”.

(4) The paleogeographic configuration, with an open connection between the east Pacific and the Caribbean across the open Central American, provides a likely setting for exposing the megabank to abnormally high nutrient levels associated with Miocene equatorial productivity. However, the specific mechanisms that have intensified nutrient supply and caused nutrification in correspondence to the drowning episodes remain unclear.

Acknowledgments

The authors thank ODP for providing the samples for this study, and acknowledge the support of Leg 165 participants. Fundings for the analytical costs for stable isotope analyses were provided by the Swiss National Science Foundation. NSF has funded cruises and post cruise research in Walton Basin and Pedro Channel (research grants OCE-8715922, -8900040, and -9116323 to A.W. Droxler, A.C. Hine, and P. Hallock). Special thanks are due to Captain Richard Ogus and the crew of the *R/V Cape Hatteras*. David Mucciarone and Timothy W. Boynton's help was invaluable in the seismic data acquisition and processing. The technical support of the Stable Isotope Laboratory in Zurich is gratefully acknowledged. Jane Teranes and Miriam Andres are thanked for their help in processing the samples. Dr. Edward Robinson (University of the West Indies, Kingston, Jamaica) provided larger benthic foraminifer-based age control for several of the dredged samples. Birgit Fabian (Potsdam) is thanked for help with the graphics. Adrian Immenhauser, Don McNeill, and Pascal Kindler are thanked for their constructive reviews.

References

- Acton GD, Galbrun B, King JW. Paleolatitudes of the Caribbean Plate since the Late Cretaceous. In: Leckie RM, Sigurdsson H,

- Acton GD, Draper G, editors. Proceeding of the Ocean Drilling Program. Scientific results, vol. 165. College Station, TX: Ocean Drilling Program; 2000. p. 149–73.
- Arden DD. Geology of Jamaica and the Nicaraguan Rise. In: Stehli FG, editor. The ocean basins and margins: the Gulf of Mexico and the Caribbean. New York: Plenum Press; 1975. p. 617–61.
- Blomeier DPG, Reijmer JGG. Drowning of a Lower Jurassic Carbonate Platform: Jbel Bou Dahar, high Atlas, Morocco. *Facies* 1999;41:81–110.
- Bryan JA, Huddleston PF. Correlation and age of the Bridgeboro limestone, a coralline limestone from southwestern Georgia. *J Paleontol* 1991;65:864–8.
- Budd AF. Long-term patterns of morphological variation within and among species of reef-corals and their relationship to sexual reproduction. *Syst Bot* 1990;15:150–65.
- Cande SC, Kent DV. Revised calibration of the geomagnetic polarity timescale for the late Cretaceous and Cenozoic. *J Geophys Res* 1995;100:6093–5.
- Carey S, Sigurdson H. Grain size of Miocene volcanic ash layers from Sites 998, 999, and 1000: implications for source areas and dispersal. In: Leckie RM, Sigurdsson H, Acton GD, Draper G, editors. Proceeding of the Ocean Drilling Program. Scientific results, vol. 165. College Station, TX: Ocean Drilling Program; 2000. p. 101–13.
- Chaisson WP, D'Hondt SL. Neogene planktonic foraminifer biostratigraphy at Site 999, western Caribbean Sea. In: Leckie RM, Sigurdsson H, Acton GD, Draper G, editors. Proceeding of the Ocean Drilling Program. Scientific results, vol. 165. College Station, TX: Ocean Drilling Program; 2000. p. 19–56.
- Cole WS. A review of American species of Miogypsinides (larger foraminifera). *Contrib Cushman Lab Foraminifer Res* 1967;18: 99–117.
- Compton JS, Snyder SW, Hodell DA. Phosphogenesis and weathering of shelf sediments from the Southeastern United States: implications for Miocene $\delta^{13}\text{C}$ excursions and global cooling. *Geology* 1990;18:99–117.
- Cunningham AD. The Neogene evolution of the Pedro Channel carbonate system, northern Nicaragua Rise. PhD thesis, Rice University, Houston; 1998.
- Droxler AW, Morse JW, Glaser KS, Haddad GA, Baker PA. Surface sediment carbonate mineralogy and water column chemistry—Nicaragua Rise versus the Bahamas. *Mar Geol* 1991;100:277–89.
- Droxler AW, Cunningham AD, Hine AC, Hallock P, Duncan D, Rosencrantz E, et al. Late middle (?) Miocene fragmentation of an Eocene–early Miocene carbonate megabank on the Northern Nicaraguan Rise tied to the tectonic activity at the North America/Caribbean plate boundary zone. AGU annual meeting, San Francisco; 1992. p. 299.
- Droxler AW, Burke K, Cunningham AD, Hine AC, Rosencrantz D, Duncan D, et al. Caribbean constraints on circulation between Atlantic and Pacific oceans over the past 40 million years. In: Burke K, editor. Tectonic Boundary Conditions for Climate Reconstruction. Oxford monographs geology and geophysics; 1998. p. 169–91.
- Duncan D, Hine AC, Droxler AW. Tectonic controls on carbonate sequence formation in an active strike-slip setting: Serranilla Basin, northern Nicaraguan Rise, Caribbean Sea. *Mar Geol* 1999;160:355–82.
- Edinger EN, Risk MJ. Oligocene–Miocene extinction and geographic restriction of Caribbean reef corals: roles of temperature, turbidity, and nutrients. *Palaios* 1994;9:576–98.
- Frank TD, Arthur MA, Dean WE. Diagenesis of Lower Cretaceous pelagic carbonates, North Atlantic: paleoceanographic signals obscured. *J Foraminifer Res* 1999;29:340–51.
- Frost SH. Cenozoic reef systems of Caribbean—prospects for paleoecological synthesis. *Studies in Geology*, vol. 4. Tulsa: Am. Ass. Petrol. Geol.; 1977. p. 93–110.
- Glaser KS, Droxler AW. High production and highstand shedding from deeply submerged carbonate banks, northern Nicaraguan Rise, Caribbean Sea. *Paleoceanography* 1991;8:243–74.
- Glaser KS, Droxler AW. Controls and development of late quaternary periplatform carbonate stratigraphy in Walton Basin (Northeastern Nicaragua Rise, Caribbean Sea). *Paleoceanography* 1993;8:243–74.
- Gomberg D. Geology of the Portales Terrace. *Fla Sci* 1974;37:15.
- Hallock P, Elrod JA. Oceanic chlorophyll around carbonate platforms in the western Caribbean; observations from CZCS data. *Int Coral Reef Symp* 1988:449–54.
- Hallock P, Schlager W. Nutrient excess and the demise of coral reefs and carbonate platforms. *Palaios* 1986;1:389–98.
- Hallock P, Hine AC, Vargo GA, Elrod JA, Jaap WC. Platforms of the Nicaraguan Rise: examples of the sensitivity of carbonate sedimentation to excess trophic resources. *Geology* 1988;16: 1104–7.
- Hine AC, Steinmetz JC. Cay Sal Bank, Bahamas—a partially drowned carbonate platform. *Mar Geol* 1984;59:135–64.
- Hine AC, Hallock P, Harris MW, Mullins HT, Belknap DF, Jaap WC. *Halimeda* bioherms along an open seaway: Meskito Channel, Nicaraguan Rise, SW Caribbean Sea. *Coral Reefs* 1988;6:173–8.
- Illing LV. Bahamian calcareous sands. *Am Assoc Pet Geol Bull* 1954;38:1–95.
- Ingle JC. Origin of diatomites around the North Pacific Rim. In: Garrison RE, Douglas RG, editors. The Monterey Formation and Related Siliceous Rocks of California. SEPM spec publ; 1981. p. 159–79.
- John CM, Karner GD, Mutti M. Delta O-18 and Marion Plateau backstripping: combining two approaches to constrain late middle Miocene eustatic amplitude. *Geology* 2004;32:829–32.
- Kameo K, Bralower TJ. Neogene calcareous nannofossil biostratigraphy of sites 998, 999, and 1000, Caribbean Sea. In: Leckie RM, Sigurdsson H, Acton GD, Draper G, editors. Proceeding of the ocean drilling program. Scientific results, vol. 165. College Station, TX: Ocean Drilling Program; 2000. p. 3–17.
- Kameo K, Sato T. Biogeography of Neogene calcareous nannofossils in the Caribbean and the eastern equatorial Pacific—floral response to the emergence of the Isthmus of Panama. *Mar Micropaleontol* 2000;39:201–18.
- Leroy S, Mecier de Lepinay B, Mauffret A, Pubellier M. Structural and tectonic evolution of the eastern Cayman Trough (Caribbean Sea) from seismic reflection data. *Am Assoc Pet Geol Bull* 1996;80:222–47.

- Mallarino G, Goldstein RH, Di Stefano P. New approaches for quantifying water depths applied to the enigma of drowning of carbonate platforms. *Geology* 2002;30:783–6.
- Matthews RK, Poore RZ. Tertiary $\delta^{18}\text{O}$ record and glacioeustatic sea-level fluctuations. *Geology* 1980;8:501–4.
- Miller KG, Fairbanks RG. Evidence for Oligocene–Miocene abyssal circulation changes in the western North Atlantic. *Nature* 1985;306:250–3.
- Miller KG, Mountain GS, Blum P, Gartner S, Alm P-G, Aubry M-P, et al. Drilling and dating New Jersey Oligocene–Miocene sequences; ice volume, global sea level, and Exxon records. *Science* 1996;271:1092–5.
- Miller KG, Mountain GS, Browning JV, Kominz M, Sugarman PJ, Christie-Blick N, et al. Cenozoic global sea level, sequences, and the New Jersey transect; results from coastal plain and continental slope drilling. *Rev Geophys* 1998;36:569–601.
- Mullins HT, Neumann AC. Geology of the Miami Terrace and its paleoceanographic implications. *Mar Geol* 1979;30:205–32.
- Mullins HT, Gardulski AF, Wise Jr SW, Applegate J. Middle Miocene oceanographic event in the eastern Gulf of Mexico: implications for seismic stratigraphic succession and Loop Current/Gulf Stream circulation. *Geol Soc Am Bull* 1987;98:702–13.
- Mutti M. Bulk $\delta^{18}\text{O}$ and $\delta^{13}\text{C}$ records from Site 999, Colombian Basin, and Site 1000, Nicaraguan Rise (latest Oligocene to middle Miocene): diagenesis, link to sediment parameters, and paleoceanography. In: Leckie RM, Sigurdsson H, Acton GD, Draper G, editors. *Proceeding of the Ocean Drilling Program. Scientific results, vol. 165. College Station, TX: Ocean Drilling Program; 2000. p. 275–83.*
- Mutti M, Bernoulli D, Stille P. Temperate carbonate platform drowning linked to Miocene oceanographic events: Maiella platform margin, Italy. *Terra Nova* 1997;9:122–5.
- Mutti M, Bernoulli D, Spezzaferri S, Stille P. Lower and Middle Miocene carbonate facies in the Central Mediterranean: the impact of paleoceanography on sequence stratigraphy. In: Harris PM, Saller AH, Simo JA, editors. *Advances in Carbonate Sequence Stratigraphy—Application to Reservoirs, Outcrops and Models. SEPM spec publ; 1999. p. 371–84.*
- Popenoe P. Cenozoic depositional and structural history of the North Atlantic margin from seismic stratigraphic analyses. In: Poag CW, editor. *Geologic Evolution of the United States Atlantic Margin. New York: Van Nostrand Reinhold; 1985. p. 125–87.*
- Prentice ML, Matthews RK. Cenozoic ice-volume history: development of a composite oxygen isotope record. *Geology* 1988;16:963–6.
- Raffi I, Flores J-A. Pleistocene through Miocene calcareous nannofossils from eastern equatorial Pacific Ocean. In: Pisias NG, Mayer LA, Janecek TR, Palmer-Julson A, van Andel TH, editors. *Proceeding of the Ocean Drilling Program. Scientific results, vol. 138. College Station, TX: Ocean Drilling Program; 1995. p. 233–86.*
- Roberts HH, Murray SP. Controls on reef development and the terrigenous–carbonate interface on a shallow shelf, Nicaragua (Central America). *Coral Reefs* 1983;2:711–80.
- Robinson E. Jamaica. In: Jackson TA, editor. *Caribbean geology: an introduction. Kingston: UWIPA; 1994. p. 111–27.*
- Roth JM, Droxler AW, Kameo K. The Caribbean Carbonate Crash at the middle to late Miocene transition: linkage to the establishment of the modern global ocean conveyor. In: Leckie RM, Sigurdsson H, Acton GD, Draper G, editors. *Proceeding of the Ocean Drilling Program. Scientific results, vol. 165. College Station, TX: Ocean Drilling Program; 2000. p. 249–73.*
- Savin SM, Woodruff F. Isotopic evidence for temperature and productivity in the Tertiary oceans. In: Riggs SR, editor. *Phosphate Deposits of the World: Neogene to Modern Phosphorites. Cambridge University Press; 1990. p. 241–59.*
- Savin SM, Douglas RG, Stehli FG. Tertiary marine paleotemperatures. *Geol Soc Am Bull* 1975;86:1499–510.
- Schlager W. The paradox of drowned reefs and carbonate platforms. *Geol Soc Am Bull* 1981;92:197–211.
- Schlager W. Scaling of sedimentation rates and drowning of reefs and carbonate platforms. *Geology* 1999;27:183–6.
- Shackleton NJ, Kennett JP. Paleotemperature history of the Cenozoic and initiation of Antarctic glaciation: oxygen and carbon isotopic analyses in DSDP sites 277, 279, and 281. In: Houtz RE, editor. *Proceeding of the deep sea drilling program, initial results. Ocean drilling program, vol. 29; 1975. p. 743–55.*
- Shackleton NJ, Hall MA, Pate D, Meynadier L, Valet P. High-resolution stable isotope stratigraphy from bulk sediment. *Paleoceanography* 1993;8:141–8.
- Sigurdson H, Leckie RM, Acton GD. *Proceeding of the Ocean Drilling Program. Initial reports, vol. 165. College Station, TX: Ocean Drilling Program; 1997. p. 743–55.*
- Triffleman NJ, Hallock P, Hine AC, Peebles MW. Morphology, sediments, and depositional environments of a small carbonate platform: Serranilla Bank, Nicaraguan Rise, Southwest Caribbean Sea. *J Sediment Petrol* 1992;62:591–606.
- Vincent E, Berger WH. Carbon dioxide and polar cooling in the Miocene: the Monterey hypothesis. In: Broecker WS, editor. *Natural variations in carbon dioxide and the carbon cycle. Am Geophys Union Monogr; 1985. p. 455–68.*
- Wilson PA, Jenkyns HC, Elderfield H, Larson RL. The paradox of drowned carbonate platforms and the origin of Cretaceous Pacific guyots. *Nature* 1988;392:889–94.
- Woodruff F, Savin SM. Miocene deepwater oceanography. *Paleoceanography* 1989;6:755–806.
- Wright JD, Miller KG, Fairbanks RG. Early and Middle Miocene stable isotopes: implications for deepwater circulation and climate. *Paleoceanography* 1992;7:357–89.
- Zachos J, Flower BP, Paul H. Orbitally paced climate oscillations across the Oligocene/Miocene boundary. *Nature* 1997;388:567–70.
- Zachos J, Pagani M, Sloan L, Thomas E, Billups K. Trends, rhythms, and aberrations in global climate 65 Ma to present. *Science* 2001;292:686–93.